Intraoperative Swept-Source OCT–Based Corneal Topography for Measurement and Analysis of Stromal Surface After Epithelial Removal

Wen Zhou, MD, MSc; Dan Z. Reinstein, MD, DABO, FRCOphth; Timothy J. Archer, MA(Oxon), DipCompSci(Cantab), PhD; Xiangjun Chen, MD, PhD; Tor Paaske Utheim, MD, PhD; Yue Feng, MD, MSc; Aleksandar Stojanovic, MD, PhD

From the Institutes of Clinical Medicine (WZ, AS) and Community Medicine (YF), Faculty of Health Sciences, University of Tromsø, Tromsø, Norway; Eye Department, University Hospital Northern Norway, Tromsø, Norway (AS); London Vision Clinic, London, United Kingdom (DZR, TJA); Columbia University Medical Center, New York, New York (DZR); Sorbonne Université, Paris, France (DZR); Biomedical Science Research Institute, Ulster University, Coleraine, United Kingdom (DZR); the Department of Ophthalmology, Arendal Hospital, Arendal, Norway (XC); and the Department of Ophthalmology, Oslo University Hospital, Oslo, Norway (TPU).

Submitted: October 1, 2020; Accepted: March 9, 2021

Disclosure: Dr. Reinstein is a consultant for Carl Zeiss Meditec AG and has a proprietary interest in the Artemis Insight 100 technology (ArcScan, Inc) through patents administered by the Cornell Center for Technology Enterprise and Commercialization (CCTEC), Ithaca, New York. The remaining authors have no proprietary or financial interest in the materials presented herein.

Acknowledgments: The authors thank Filip Stojanovic, MD, for his contributions to the article.

Correspondence: Aleksandar Stojanovic, MD, PhD, Eye Department, University Hospital North Norway, Sykehusveien 38, 9019 Tromsø, Norway. Email: aleks@online.no

doi:10.3928/1081597X-20210405-01

ABSTRACT

PURPOSE: To assess intraoperative stromal topography measurements using swept-source optical coherence tomography (OCT)–based topography/tomography after epithelial removal and to analyze the epithelial contribution to the corneal topography and optics.

METHODS: This was a prospective series of 22 eyes of 19 patients referred to receive phototherapeutic keratotomy (PTK) for treatment of recurrent corneal erosion and a control group of 22 virgin eyes. Swept-source OCT corneal topography/tomography was obtained immediately before and immediately after mechanical deepithelialization before PTK. Epithelial thickness maps were obtained before the surgery using spectral-domain OCT in the control group and as a reference in the group with anterior basement membrane dystrophy. Topographic and optical characteristics, including the curvature, astigmatism, asphericity, and higher order aberrations of the cornea before and after deepithelialization were compared, and their differences correlated with the measurements derived from the epithelial thickness maps.

RESULTS: Stromal topography measurements after deepithelialization were easily obtained and showed excellent repeatability. Assessment of corneal edema induced by deepithelialization revealed that it did not significantly affect the measured parameters. The stromal surface was steeper by 1.28 diopters, had higher with-the-rule astigmatism by 0.41 diopters, was more prolate, and had more higher order aberrations compared to the intact epithelialized corneal surface. These differences correlated well with the parameters derived from epithelial thickness maps.

CONCLUSIONS: Measurement of stromal topography using swept-source OCT immediately after mechanical deepithelialization may be a viable method in therapeutic refractive surgery, where stromal topography-guided ablation is needed. A significant epithelial contribution to anterior corneal topography and optics was confirmed.

As the refractive medium with direct contact with the air, the corneal epithelium plays a significant role in the ocular refractive system. Even if the epithelium had a uniform thickness profile and a refractive index identical to that of the stroma, its sheer removal would increase the refractive power of the cornea due to the shortening of the radius of curvature.[1] In fact, the corneal epithelium has a higher refractive index (1.401) than the anterior stroma (1.380), a difference sufficient to affect overall corneal power.[2] Additionally, the epithelium has a non-uniform thickness profile due to the effect of eyelid blinking mechanics,[3,4] and the inherent behavior of epithelial cells to smooth the underlying stromal surface irregularities.[4-8] The epithelial thickness profile can produce myopic, hyperopic, astigmatic, and higher order aberration (HOA) shifts in the corneal optics.[4,9] The epithelial thickness profile can also be influenced by other factors, including anterior basement membrane dystrophy (ABMD)[10] and dry eye.[11] Epithelial remodeling may be sufficient to fully mask the stromal surface irregularity, as has been shown in the detection of keratoconus with normal topography.[3,4,8,12] This compensatory function means that anterior surface topography can be poorly representative of underlying stromal irregularity, resulting in poor outcomes of topography-guided therapeutic surgery and pointing to the need for transepithelial phototherapeutic keratotomy (PTK) and topography-guided ablation to achieve stromal regularization.[9,13-16] Reinstein et al[17] used epithelial thickness maps to generate stromal topography and performed the first stromal topography-guided treatment, whereas Vinciguerra et al[18,19] used intraoperative stromal topography to plan sequential stromal topography-guided treatment. Studies using either direct measurement of the corneal stromal surface immediately after epithelial debridement,[1,20-23] mathematically modeled stromal/Bowman's layer surface,[24] or Bowman's layer topography constructed by edge detection of the surface of Bowman's layer on 12 radial corneal swept-source optical coherence tomography (SS-OCT) B-scans[25] have also shown variation in epithelial and stromal topographic and optical characteristics.

The purpose of the current study was to assess the viability of SS-OCT technology for intraoperative measurement of stromal topography after epithelial removal. We also intended to compare the corneal anterior and stromal topographic and optical characteristics acquired by SS-OCT–based topography between the eyes with ABMD and the control group of virgin eyes, as well as to quantify the corneal epithelial contribution to the corneal topography and optics in the ABMD group.

PATIENTS AND METHODS

This prospective study included 22 eyes of 19 patients with ABMD referred for PTK for treatment of recurrent corneal erosion at the Eye Department of the University Hospital of North Norway from April 2015 to March 2019. A control group of 22 healthy virgin eyes of 22 consecutive candidates for elective laser vision correction at the SynsLaser clinic in Tromsø, Norway.

Only eyes with intact epithelium on slit-lamp examination, normal epithelial distribution on epithelial thickness map, and no history of corneal erosion at least 1 month before the PTK surgery were included. Patients presenting with ocular pathology other than the history of recurrent corneal erosions and eyes that had undergone previous ocular surgery were excluded from the study. Soft contact lens users were instructed to stop using the lenses 1 week before the measurements; no hard contact lens users were included. The study was approved by the Norwegian Regional Committee for Medical & Health Research Ethics (REK-Nord 2014/1401). All patients provided informed consent for the anonymous use of their data in scientific analyses and publications. Standard preoperative ocular examination, including slit-lamp biomicroscopy, visual acuity/subjective manifest refraction, and fundus examinations were performed in all eyes. An SS-OCT–based topographer/tomographer (Casia SS- 1000; Tomey Corporation) was used for corneal topography and a spectral-domain OCT (SD-OCT) scanner (RTVue-100; Optovue, Inc) was used for the epithelial thickness maps. To limit the influence of overnight swelling,[26] the measurements were performed at least 4 hours after the patients awoke.

The Casia SS-1000 was located approximately 1 meter away from the surgery bed. Initial topography with SS-OCT was obtained before the application of 0.5% proparacaine anesthetic drops (Alcaine; Alcon

Laboratories, Inc). The patients were asked to blink three times before each of the three acquisitions, and the average value was used for further analyses. The epithelium was then removed completely over the central 9 mm of the corneal surface using an electric epithelial scrubber (Amoils brush; Innovative Excimer Solutions). The surgeon exercised special care in removing the epithelium in the gentlest but most thorough manner to leave an intact and smooth Bowman's membrane. The corneal surface was rinsed with a balanced salt solution (BSS; Alcon Laboratories, Inc) and inspected under the microscope to ensure that all epithelial debris had been removed. After the deepithelialization and before the final PTK procedure, the patients were asked to move to the Casia SS-1000 again to undergo another three acquisitions of the topographies. The patients were asked to blink before each acquisition. No artificial tears were necessary to enhance the examination and the corneas were not dried before the acquisition. The raw OCT data and the instrument's edge-detection processing of each image were checked for artifacts. A bandage contact lens (Acuvue Oasys; Johnson & Johnson) was placed over the eye after the PTK procedure had been completed.

Measurements

The Casia SS-1000 automatically moves the chinrest until the patient's eye reaches the correct position and initiates 0.34-second long acquisition, with the reference axis of the measurements aligned with the corneal vertex.[27,28] The analysis software identifies the anterior and posterior corneal surfaces and generates the corneal pachymetry, elevation, curvature, and refractive maps. We compared the following topographic and optical parameters of the anterior corneal (epithelium-covered) surface and the stromal (deepithelialized) surface: (1) radius of the best-fit sphere (BFS) at the 3.5-, 6-, and 9-mm zones; (2) radius of the axial curvature and its orientation along the steepest and flattest meridians at the 3.5-mm zone; (3) corneal asphericity (mean Q-value) measured over the central 6-mm zone; and (4) Fourier HOAs measured over the central 3- and 6-mm zones.

In addition, the BFS radius of the posterior corneal surface at the 3.5-, 6-, and 9-mm zones, and the pachymetry at the corneal vertex before and after deepithelialization were also analyzed. The amount of edema induced by the deepithelialization was expressed as the difference between the reduced pachymetry after deepithelialization and the epithelial thickness measured by SD OCT preoperatively (amount of central edema = preoperative central epithelial thickness – [central $\text{pachymetry}_{\text{epi-on}}$ – central $\text{pachymetry}_{\text{epi-off}}$]).

Preoperative epithelial thickness map measurements by SD-OCT, centered on the corneal vertex, covering the central 6-mm diameter zone, were also performed. Three consecutive acquisitions were performed for each eye. Auto-generated averaged regional epithelial thickness was recorded for the following areas: central 2 mm and paracentral 2- to 5-mm ring divided into superior, superior temporal, temporal, temporal inferior, inferior, inferior nasal, nasal, and superior nasal sectors.

Contribution of the Epitheliumto the Refractive Power

To evaluate the dioptric refractive power contribution of the epithelium, radii of the anterior cornea with epithelium-on and the stromal surface after epithelial removal were converted to power. According to the law of Gaussian optics, the following formula was used for the two interfaces: Power = $(n' - n)/r$, where n and n' are the refractive index of the media in front and behind the refractive interface, respectively, and r is the radius of the interface curvature measured by the Casia SS-1000. The refractive indexes used for the epithelium and anterior stroma were 1.401 and 1.380, respectively.[2] Considering the epithelium as a thin refractive lens with two refractive interfaces (air–epithelium interface and epithelium– stroma interface), the power of the "epithelium lens" residing between air and the stroma is represented by $\text{power}_{\text{air-epithelium}} + \text{power}_{\text{epithelium-stroma}} - \text{power}_{\text{air-stroma}}$.

Evaluation of Astigmatism

The axial radii and their orientation along the steepest and flattest meridians within the anterior diameter of 3.5 mm, with and without epithelium, were recorded for evaluating astigmatism. The radii were converted to power values using the law of Gaussian optics. The axis and power of astigmatism were calculated for the air– epithelium interface, epithelium–stroma interface, and air–stroma interface. The astigmatism values were then decomposed into two Jackson cross-cylinder lenses, one with power J0 = (– C/2) cos (2a) at axis a = 0 = 180 degrees, and the other with power J45 = (– C/2) sin (2a) at axis a = 45 degrees, for further comparison.[29] In this representation, an increase in J0 indicates an increased component of with-the-rule (WTR) astigmatism or decreased component of against-the-rule (ATR) astigmatism, and vice versa. A change in J45 indicates a change in oblique astigmatism. The contribution of the epithelium to astigmatism was calculated as:

$$\sqrt{(J0 + J0' - J0'')^2 + (J45 + J45' - J45'')^2}$$

where J0 and J45, J0' and J45', and J0" and J45" represent the Jackson cross-cylinder components of astigmatism for the air–epithelium, epithelium–stroma, and air–stroma interface, respectively. For vector summation, air–epithelium and air–stroma interface astigmatism were defined using the negative magnitude and flat axis. Because the epithelium–stroma interface has a divergent optical effect, epithelium–stroma interface astigmatism was also defined with a negative magnitude but using the steep axis for vector addition.

Statistical Analysis

Statistical analysis was performed using SPSS Statistics 24 (IBM Corporation). The normal distribution of continuous variables was confirmed using the Kolmogorov-Smirnov test and Q-Q plot. The paired *t* test and related-samples Wilcoxon signed-rank test were used for comparing the epithelium-on and epithelium-off parameters with normal and non-normal distribution, respectively. The Pearson correlation and Spearman rank correlation were used for defining the correlation between parameters with normal and non-normal distribution, respectively. A *P* value of less than .05 was considered statistically significant.

RESULTS

The 22 topographies before and after deepithelialization, and the preoperative epithelial thickness maps, were from 7 women (36.8%) and 12 men (63.2%). The mean patient age was 46.21 ± 13.18 years (range: 25 to 70 years). The measured parameters and calculated values for the epithelial and stromal surfaces are listed in Table 1. The patients' demographic and topographic data were comparable to those of the 22 normal virgin eyes in the control group (Table A, available in the online version of this article). The correlation between the deepithelialization-induced changes and the epithelial thickness in different areas are listed in Table B (available in the online version of this article). Preoperative epithelial thickness distribution over the central 5-mm diameter of the ABMD and control groups is shown in Figure 1. The average epithelial thickness profile was similar between groups, with both showing thicker epithelium inferiorly compared to superiorly. This difference was greater in the ABMD group (6.00 μm) compared to the control group (2.08 μm). The epithelial thickness was thicker in the ABMD group in the central and inferior zones, as shown in Figure 2.

The best-fit sphere (BFS) radius of the anterior corneal surface (epithelium-covered) was significantly larger at both the 3.5- and 6-mm diameter zone compared to that of the stromal surface (measured after deepithelialization), whereas the opposite was true at the 9-mm diameter zone. The difference in the BFS radius between the two surfaces at the 3.5-mm diameter showed a statistically significant correlation with the paracentral 2 to 5 mm epithelial thickness ($P = .011$, $R = 0.571$). Compared to the stromal surface, the anterior corneal surface had lower prolateness at the 6-mm diameter zone, and lower HOAs at both the 3- and 6-mm diameter zone. Asphericity between the epithelial and stromal surfaces was correlated with paracentral epithelial thickness ($P = .039$, $R = 0.477$). The difference in HOAs at the 3-mm diameter zone was correlated with the standard deviation of the epithelial thickness profile ($P = .041$, $R = -0.472$).

There was no statistically significant change in the BFS radius of the posterior corneal surface at the 3.5- and 6-mm diameter zone after epithelial debridement, whereas the BFS radius at the 9-mm diameter zone was significantly increased after deepithelialization ($P < .001$).

The astigmatism contribution of the "epithelium lens" between the air and the stroma was -0.25 D × 7, whereas the astigmatism for the air–stroma interface after deepithelialization was -1.04 D ×178, yielding epithelium-induced astigmatism of -0.76 D × 85 (Figure 3). The average central epithelial thickness before debridement was 57.42 ± 3.55 μm, whereas the mean variation of central corneal thickness before and after deepithelialization was 37.95 ± 7.95 μm, indicating an average central stromal thickening of 19.47 ± 7.09 μm, which was interpreted as stromal edema. The stromal edema was not correlated with any of the measured parameters on the anterior cornea, whereas the amount of flattening of the posterior cornea at the 9-mm diameter zone after deepithelialization showed a significant correlation with the amount of stromal edema ($P = .027$, $R = 0.482$).

The intraclass correlation coefficients of three consecutive measurements for each anterior curvature parameter before and after epithelial removal were high, ranging between 0.993 and 0.999, and are summarized in Table C (available in the online version of this article.

DISCUSSION

We found SS-OCT technology capable of producing measurements of stromal topography after epithelial removal, as well as repeatable and convenient for use in therapeutic refractive surgery in cases where intraoperative stromal mapping after deepithelialization is necessary. We also looked at the epithelial contribution to the corneal optics by studying SS-OCT topographies before and after deepithelialization in eyes with ABMD. We found that the epithelial contribution to the total corneal power consisted of negative optical power, positive asphericity, and HOAs that are inverse to the stromal aberrations. These findings are in accord with the literature,[22,23] as is the comparison of the epithelial thickness maps between eyes with ABMD and virgin eyes, showing thicker central and inferior epithelium in the ABMD group.[10]

As Reinstein et al[4] described in 2008, epithelium in normal eyes is not a layer with uniform thickness and there is also a variation in thickness distribution between two eyes of the same person. The epithelial thickness was found to be distributed according to the stromal surface curvature gradient and the template provided by the eyelid.[4,13,15,16,30-32] The superior-inferior asymmetry in the average epithelial thickness profile found in the current study was similar to that previously reported and the thinner superior epithelium is most likely due to the influence of the upper eyelid.

To study the topographic and optical contribution of the epithelium, we used direct stromal topography obtained immediately after deepithelialization and correlated it to the anterior corneal topography obtained by the same device right before deepithelialization. It is difficult to accurately measure the stromal topography of newly deepithelialized cornea via Placido-based, scanning-slit-based,[33] or PAR Corneal Topography,[34,35] The reason may be that these technologies use an intense visible examination light, which causes photophobia, involuntary ocular movements, and hence improper patient fixation after deepithelialization. In the current study, the deepithelialized corneas were exposed to SS-OCT infrared light of 1,300-nm wavelength, which is not visible to the patient. It also allows better penetration into an opaque cornea[36] compared to visible light. The short topography acquisition time additionally reduces patient discomfort and may contribute to minimizing motion artifacts resulting from ocular movement. Finally, the instrument uses a quick software-controlled alignment system, which automatically moves the unit to the measurement position according to the corneal reflex,[28] making examination possible even under the most difficult conditions. It should be noted that the tear film, which is normally registered as the first corneal surface by OCT-based topography, has a smoothing effect on the corneal curvature, introducing a potential measurement error, especially in highly irregular cases.

In 1993, Simon et al[1] published an evaluation of surface topography before and after deepithelialization to determine epithelial power in human cadaver eyes. Measurement of corneal topographic changes after epithelial debridement in normal myopic eyes or keratoconic eyes has also been reported based on the use of either high-frequency digital ultrasound,[24] anterior elevation,[17] or Placido topography.[20-22] The Triton SS-OCT scanner (Topcon, Inc) has also been used for noncontact quantification of topography of the anterior corneal surface and Bowman's layer.[25] Most of these studies concluded that the epithelium tends to reduce corneal curvature,[1,21,22,24,25] magnitude of astigmatism,[20,22,25] irregularities,[20,21] and prolateness.[1,20,22] Our results concur, demonstrating that the epithelium-on corneal surface was significantly flatter, and had lower magnitude of astigmatism and decreased HOAs and prolateness compared to the measurements after deepithelialization. These differences correlated well with the parameters derived from epithelial thickness maps in the same group of eyes obtained before deepithelialization (Table B). Figure A (available in the online version of this article) shows the difference between the elevation topographies before and after deepithelialization alongside the epithelial thickness map of the same eye before deepithelialization. The epithelial profile can be seen to account for the asymmetric difference in elevation topography. Our general conclusions concerning the stromal topography and epithelial contribution to the corneal optics for both groups in the current study were in agreement and comparable with previously published similar studies.[1,20-22,24]

Stromal edema was seen to occur after epithelial debridement in all of our cases, with a mean central increase in stromal thickness value of 19.47 ± 7.09 μm. Gatinel et al[20] reported a central corneal thickness difference of 37.84 ± 9.82 μm after deepithelialization, which amounts to approximately 15 μm of stromal edema, if subtracted from the average epithelial thickness of 53 μm, as published by Reinstein et al[3] using the gold standard of very high-frequency digital ultrasound. Potential measurement errors in curvature measurements caused by stromal edema were a concern, but we found that changes in central stromal thickness were not correlated with the measured curvature parameters of the anterior cornea; However, we did find a significant correlation with the amount of posterior corneal flattening at the 9-mm diameter zone. This result is in accordance with the findings of Meek et al,[37] who reported that fluid entering the cornea causes more swelling in the posterior lamellae than in the anterior lamellae, explained by the lamellar interweaving and their insertion into Bowman's layer, as well as the differences in the glycosaminoglycans in the anterior and posterior stroma. In addition, in vitro studies have shown that substantial corneal hydration may cause statistically significant but clinically minimal change in the anterior corneal curvature.[38,39]

One inclusion criterion in the ABMD group was a healthy epithelium on slit-lamp examination and normal epithelial thickness distribution on epithelial thickness map. The recurrent erosion syndrome group had symptoms of recurrent corneal erosion without signs. Our control group of healthy virgin eyes with no symptoms of recurrent erosion was recruited from candidates for elective laser vision correction. Table 2 shows no significant difference between the groups in terms of preoperative central pachymetry, radius of anterior BFS, and anterior asphericity. However, the group representing eyes with ABMD showed thicker epithelium generally and a greater inferior-superior difference, as shown on Figures 1-2. Buffault et al10 recently published similar findings. This observation is as expected: ABMD results in duplication of the basement membrane of the epithelium with abnormalities and alteration in the heathy columnar organization from cuboidal basal cells to wing-cells and then flattened squamous cells. It is thus expected that the epithelial thickness profile of eyes with ABMD will be different from that of a normal cornea.

Current surface ablation treatments are performed on the deepithelialized stromal surface, whereas the ablation parameters have been based on the corneal topography and refractive measurements before deep-ithelialization. The differences in topography of the two surfaces and the optical influence of the epithelium have been modelled to result in ablation errors, the average of which is nomogram-compensated in normal regular corneas.[40,41] In the case of irregular corneas, the epithelium will be even more irregular, explaining why transepithelial topography-guided procedures are more effective for repairing irregular corneas than stromal ablations based on topography alone.[14-16,42] In transepithelial topography-guided surgery, the transepithelial PTK component treats the irregularity masked by the epithelium and the topography-guided

component treats the remainder. Also, the empirically derived preset ablation rate and epithelial thickness compensations may be a source of ablation depth errors[43] in irregular cases. Transepithelial topography-and epithelial thickness map–guided PRK may provide improved accuracy, although there will be a high demand on the treatment laser's scanning resolution and its tracking precision that may be beyond the currently available technology. Transepithelial PTK does not require this level of tracking accuracy. Alternatively, direct stromal topography-guided treatments have been demonstrated. In the first, Reinstein et al[17] obtained stromal topography maps by subtracting the very high-frequency digital ultrasound-derived epithelial thickness profile from the corneal front surface elevation data, derived from scanning slit tomography (Orbscan; Bausch & Lomb), and used this to perform a custom stromal surface topography-guided laser in situ keratomileusis (LASIK) enhancement following a short flap LASIK complication. The second method described by Vinciguerra et al[19] used intraoperative stromal topography measurements after deepithelialization to perform stromal topography–based wavefront-guided ablation.

Anterior segment OCT technology has lately undergone rapid development.[44] Current SD-OCT instruments produce good epithelial thickness maps, but not topography, whereas the SS-OCT instruments produce excellent topography, but not epithelial thickness maps. Currently, the only hybrid topographer/tomographer is the MS-39 (CSO). The MS39 obtains the front surface topography by combining the instantaneous Placido ring–derived surface with auto-correlated rotational corneal SD-OCT scanning technology, allowing the back surface to be calculated by using the highly accurate thickness measurements "hanging" from the aforementioned anterior surface. A second device, an ultra-thin blue laser scanner imaging topographer/tomographer (Precisio2; iVIS), is currently able to deliver both topography and epithelial thickness mapping. These devices may be in an excellent position to allow for stromal topography– guided ablation planning.

Noncontact quantification of topography of Bowman's layer on the intact corneas using SS-OCT[25] and SD-OCT[45] has already been reported. We have demonstrated the viability of stromal topography measurements with SS-OCT measured intraoperatively on deepithelialized stroma, a method appropriate for use in therapeutic refractive surgery in cases with significant epithelial opacity and/or defects where deepithelialization is planned as part of the treatment procedure.

AUTHOR CONTRIBUTIONS

Study concept and design (WZ, XC, TPU, AS); data collection (WZ, YF); analysis and interpretation of data (WZ, DZR, TJA, AS); writing the manuscript (WZ, YF); critical revision of the manuscript (WZ, XC, DZR, TJA, TPU); statistical expertise (WZ, DZR, TJA); supervision (XC, TPU, AS)

REFERENCES

1. Simon G, Ren Q, Kervick GN, Parel JM. Optics of the corneal epithelium. *Refract Corneal Surg*. 1993;9(1):42-50.
2. Patel S, Marshall J, Fitzke FW 3rd. Refractive index of the human corneal epithelium and stroma. *J Refract Surg*. 1995;11(2):100- 105.
3. Reinstein DZ, Silverman RH, Coleman DJ. High-frequency ultrasound measurement of the thickness of the corneal epithelium. *Refract Corneal Surg*. 1993;9(5):385-387.
4. Reinstein DZ, Archer TJ, Gobbe M, Silverman RH, Coleman DJ. Epithelial thickness in the normal cornea: three-dimensional display with Artemis very high-frequency digital ultrasound. *J Refract Surg*. 2008;24(6):571-581. doi:10.3928/108159

7X-20080601-05
5. Reinstein DZ, Archer TJ, Gobbe M. Change in epithelial thickness profile 24 hours and longitudinally for 1 year after myopic LASIK: three-dimensional display with Artemis very high-frequency digital ultrasound. *J Refract Surg*. 2012;28(3):195-201. doi:10.3928/1081597X-20120127-02
6. Maloney RK. Is corneal contour influenced by tension in the superficial epithelial cells? *Refract Corneal Surg*. 1993;9(2):147.
7. Huang D, Tang M, Shekhar R. Mathematical model of corneal surface smoothing after laser refractive surgery. *Am J Ophthalmol*. 2003;135(3):267-278. doi:10.1016/S0002-9394(02)01942-6
8. Reinstein DZ, Archer TJ, Gobbe M. Corneal epithelial thickness profile in the diagnosis of keratoconus. *J Refract Surg*. 2009;25(7):604-610. doi:10.3928/1081597X-20090610-06
9. Reinstein DZ, Archer TJ, Gobbe M. Refractive and topographic errors in topography-guided ablation produced by epithelial compensation predicted by 3D Artemis VHF digital ultrasound stromal and epithelial thickness mapping. *J Refract Surg*. 2012;28(9):657-663. doi:10.3928/1081597X-20120815-02
10. Buffault J, Zéboulon P, Liang H, et al. Assessment of corneal epithelial thickness mapping in epithelial basement membrane dystrophy. *PLoS One*. 2020;15(11):e0239124. doi:10.1371/journal.pone.0239124
11. Abou Shousha M, Wang J, Kontadakis G, et al. Corneal epithelial thickness profile in dry-eye disease. *Eye (Lond)*. 2020;34(5):915-922. doi:10.1038/s41433-019-0592-y
12. Reinstein DZ, Archer TJ, Gobbe M. Stability of LASIK in topographically suspect keratoconus confirmed non-keratoconic by Artemis VHF digital ultrasound epithelial thickness mapping: 1-year follow-up. *J Refract Surg*. 2009;25(7):569-577. doi:10.39 28/1081597X-20090610-02
13. Reinstein DZ, Archer TJ, Gobbe M. Improved effectiveness of transepithelial PTK versus topography-guided ablation for stromal irregularities masked by epithelial compensation. *J Refract Surg*. 2013;29(8):526-533. doi:10.3928/1081597X-20130719-02
14. Chen X, Stojanovic A, Zhou W, Utheim TP, Stojanovic F, Wang Q. Transepithelial, topography-guided ablation in the treatment of visual disturbances in LASIK flap or interface complications. *J Refract Surg*. 2012;28(2):120-126. doi:10.3928/10815 97X-20110926-01
15. Reinstein DZ, Archer T. Combined Artemis very high-frequency digital ultrasound-assisted transepithelial phototherapeutic keratectomy and wavefront-guided treatment following multiple corneal refractive procedures. *J Cataract Refract Surg*. 2006;32(11):1870-1876. doi:10.1016/j.jcrs.2006.07.016
16. Reinstein DZ, Archer TJ, Dickeson ZI, Gobbe M. Transepithelial phototherapeutic keratectomy protocol for treating irregular astigmatism based on population epithelial thickness measurements by Artemis very high-frequency digital ultrasound. *J Refract Surg*. 2014;30(6):380-387. doi:10.3928/10815 97X-20140508-01
17. Reinstein DZ, Gobbe M, Archer TJ, Youssefi G, Sutton HF. Stromal surface topography-guided custom ablation as a repair tool for corneal irregular astigmatism. *J Refract Surg*. 2015;31(1):54- 59. doi:10.3928/1081597X-20141218-06
18. Vinciguerra P, Camesasca FI, Morenghi E, et al. Corneal apical scar after hyperopic excimer laser refractive surgery: long-term follow-up of treatment with sequential customized therapeutic keratectomy. *J Refract Surg*. 2018;34(2):113-120. doi:10.3928/1 081597X-20171214-01
19. Vinciguerra P, Camesasca FI. Custom phototherapeutic keratectomy with intraoperative topography. *J Refract Surg*. 2004;20(5):S555-S563. doi:10.3928/1081-597X-20040901-28
20. Gatinel D, Racine L, Hoang-Xuan T. Contribution of the corneal epithelium to anterior corneal topography in patients having myopic photorefractive keratectomy. *J Cataract Refract Surg*. 2007;33(11):1860-1865. doi:10.1016/j.jcrs.2007.06.041
21. Touboul D, Trichet E, Binder PS, Praud D, Seguy C, Colin J. Comparison of front-surface corneal topography and Bowman membrane specular topography in keratoconus. *J Cataract Refract Surg*. 2012;38(6):1043-1049. doi:10.1016/j.jcrs.2012.01.026
22. Salah-Mabed I, Saad A, Gatinel D. Topography of the corneal epithelium and Bowman layer in low to moderately myopic eyes. *J Cataract Refract Surg*. 2016;42(8):1190-1197. doi:10.1016/j.jcrs.2016.05.009
23. Ziaei M, Meyer J, Gokul A, Vellara H, McGhee CNJ. Direct measurement of anterior corneal curvature changes attributable to epithelial removal in keratoconus. *J Cataract Refract Surg*. 2018;44(1):71-77. doi:10.1016/j.jcrs.2017.10.044

24. Patel S, Reinstein DZ, Silverman RH, Coleman DJ. The shape of Bowman's layer in the human cornea. *J Refract Surg*. 1998;14(6):636-640.
25. Matalia H, Francis M, Gangil T, et al. Noncontact quantification of topography of anterior corneal surface and Bowman's layer with high-speed OCT. *J Refract Surg*. 2017;33(5):330-336. doi:1 0.3928/1081597X-20170201-01
26. Feng Y, Varikooty J, Simpson TL. Diurnal variation of corneal and corneal epithelial thickness measured using optical coherence tomography. *Cornea*. 2001;20(5):480-483. doi:10.1097/00003226-200107000-00008
27. Miura M, Mori H, Watanabe Y, et al. Three-dimensional optical coherence tomography of granular corneal dystrophy. *Cornea*. 2007;26(3):373-374. doi:10.1097/ICO.0b013e31802e1e50
28. Nakagawa T, Maeda N, Higashiura R, Hori Y, Inoue T, Nishida K. Corneal topographic analysis in patients with keratoconus using 3-dimensional anterior segment optical coherence tomography. *J Cataract Refract Surg*. 2011;37(10):1871-1878. doi:10.1016/j.jcrs.2011.05.027
29. Thibos LN, Horner D. Power vector analysis of the optical outcome of refractive surgery. *J Cataract Refract Surg*. 2001;27(1):80-85. doi:10.1016/S0886-3350(00)00797-5
30. Reinstein DZ, Archer TJ, Gobbe M, Kanellopoulos AJ, Asimellis G. Rate of change of curvature of the corneal stromal surface drives epithelial compensatory changes and remodeling. *J Refract Surg*. 2014;30(12):799-802. doi:10.3928/108159 7X-20141113-02
31. Vinciguerra P, Roberts CJ, Albé E, et al. Corneal curvature gradient map: a new corneal topography map to predict the corneal healing process. *J Refract Surg*. 2014;30(3):202-207. doi:10 .3928/1081597X-20140218-02
32. Vinciguerra P, Azzolini C, Vinciguerra R, Kanellopoulos AJ, Asimellis G. Corneal curvature gradient determines corneal healing process and epithelial behavior. *J Refract Surg*. 2015;31(4):281-282. doi:10.3928/1081597X-20150319-08
33. Altan-Yaycioglu R, Pelit A, Akova YA. Comparison of ultrasonic pachymetry with Orbscan in corneal haze. *Graefes Arch Klin Exp Ophthalmol*. 2007;245(12):1759-1763. doi:10.1007/ s00417-007-0578-5
34. Uçakhan OO, Sternberg GJ, Sokol J, Brodie SE, Asbell PA. Is intraoperative topography predictive of postoperative topographical changes following refractive surgery? *CLAO J*. 2000;26(2):97-101.
35. Moser C, Kampmeier J, McDonnell P, Psaltis D. Feasibility of intraoperative corneal topography monitoring during photorefractive keratectomy. *J Refract Surg*. 2000;16(2):148-154.
36. Radhakrishnan S, Rollins AM, Roth JE, et al. Real-time optical coherence tomography of the anterior segment at 1310 nm. *Arch Ophthalmol*. 2001;119(8):1179-1185. doi:10.1001/ archopht.119.8.1179
37. Meek KM, Leonard DW, Connon CJ, Dennis S, Khan S. Transparency, swelling and scarring in the corneal stroma. *Eye (Lond)*. 2003;17(8):927-936. doi:10.1038/sj.eye.6700574
38. Simon G, Small RH, Ren Q, Parel JM. Effect of corneal hydration on Goldmann applanation tonometry and corneal topography. *Refract Corneal Surg*. 1993;9(2):110-117.
39. Ousley PJ, Terry MA. Hydration effects on corneal topography. *Arch Ophthalmol*. 1996;114(2):181-185. doi:10.1001/archopht.1996.01100130175011
40. Reinstein DZ, Patel S, Silverman RH, Aslanides IM, Coleman DJ. Epithelial lenticular types of the human cornea; classification and analysis of their influence in PRK. American Academy of Ophthalmology Annual Meeting; 1995; Atlanta, Georgia.
41. Reinstein DZ, Patel S, Aslanides IM, et al. Epithelial and corneal pachymetric topography in PRK: effect on pre-operative planning and post-operative refraction. Presented at: Association for Research in Vision and Ophthalmology Annual Meeting; 1995; Fort Lauderdale, Florida.
42. Zhou W, Reinstein DZ, Chen X, et al. Transepithelial topography-guided ablation assisted by epithelial thickness mapping for treatment of regression after myopic refractive surgery. *J Refract Surg*. 2019;35(8):525-33. doi:10.3928/1081597X-20190730-01
43. Goggin M, Stewart P, Andersons V, Criscenti G. Fine tuning of the default depth and rate of ablation of the epithelium in customized trans-epithelial one-step superficial refractive excimer laser ablation. *Eye Vis (Lond)*. 2019;6(1):39. doi:10.1186/ s40662-019-0159-9
44. Hwang ES, Schallhorn JM, Randleman JB. Utility of regional epithelial thickness measurements in corneal evaluations. *Surv Ophthalmol*. 2020;65(2):187-204. doi:10.1016/j.survophthal.2019.09.003

45. Khamar P, Shetty R, Ahuja P, et al. Accuracy of OCT curvature and aberrations of Bowman's layer: a prospective comparison with physical removal of epithelium. *J Refract Surg*. 2020;36(3):193-198. doi:10.3928/1081597X-20200122-01

TABLE 1
Difference in Measurements Before and After Epithelial Removal

Parameter	Before Epithelial Removal, Mean ± SD	After Epithelial Removal, Mean ± SD	*P*
Radius of BFS of anterior surface (mm)			
3.5 mm	7.70 ± 0.39	7.58 ± 0.37	< .001
6 mm	7.82 ± 0.34	7.76 ± 0.36	< .001
9 mm	7.93 ± 0.34	8.01 ± 0.34	< .001
Radius of BFS of posterior surface (mm)			
3.5 mm	6.59 ± 0.35	6.58 ± 0.32	.687
6 mm	6.63 ± 0.31	6.63 ± 0.30	.702
9 mm	6.77 ± 0.30	6.80 ± 0.29	< .001
Fourier higher order aberrations (μm)			
3 mm	0.16 ± 0.07	0.27 ± 0.15	< .001
6 mm	0.18 ± 0.07	0.33 ± 0.19	< .001
Components of anterior corneal astigmatism (D)			
J0	0.12 ± 0.47	0.52 ± 0.7	.001
J45	0.03 ± 0.43	-0.03 0.52	.281
Anterior asphericity (6 mm)	-0.25 ± 0.35	-0.63 ± 0.45	.006

SD = standard deviation; BFS = best-fit sphere

TABLE A
Demographic and Topographic/Tomographic Data in Main and Control Group

	Main Group		Control Group		
Parameter	**Mean ± SD**	**Range**	**Mean ± SD**	**Range**	***P***
Age (y)	46.21 ± 13.18	25 to 70	30.23 ± 5.85	20 to 39	< .05
Gender	36.8% female and 63.2% male		40.91% female and 59.09% male		
Eye	59.1% right eye and 40.9% left eye		50% right eye and 50% left eye		
Spherical equivalent (D)	-0.55 ± 1.35	-4.38 to 1.38	-3.00 ± 1.25	-5.13 to -1.00	< .05
Central pachymetry (μm)	545.06 ± 35.46	478 to 596	535.32 ± 27.82	489 to 599	.32
Radius of anterior BFS at 9 mm	7.93 ± 0.34	7.26 to 8.71	7.81 ± 0.27	7.42 to 8.42	.22
Anterior asphericity (6 mm)	-0.25 ± 0.35	-0.90 to 0.69	-0.07 ± 0.46	-0.57 to 0.73	.15

SD = standard deviation; BFS = best-fit sphere

TABLE B
Correlation Between the Epithelium Removal–Induced Changes and the Epithelial Thickness in Different Areas

	Epithelial Thickness				
Parameter	**Central 2 mm**	**Paracentral 2-5 mm**	**V-Ha**	**SD of Epib**	**Edema**
Radius of anterior BFS at 3.5 mm	*P* = .061	*P* = .011. *R* = 0.571, *R*2 = 0.326	*P* = .38	*P* = .184	*P* = .305
Radius of anterior BFS at 6 mm	0.569	0.435	0.200	0.765	0.827
Radius of anterior BFS at 9 mm	0.425	0.534	0.289	0.262	0.426
Anterior asphericity	0.131	0.039, *R* = 0.477, *R*2 = 0.228	0.625	0.237	0.433
Radius of posterior BFS at 9 mm	0.331	0.240	0.969	0.171	0.027, *R* = -0.482
J0	0.757	0.608	0.02, *R* = -0.529, *R*2 = 0.28	0.842	0.948
HOAs at 3 mm	0.558	0.283	0.657	0.041, *R* = -0.472	0.219
HOAs at 6 mm	0.751	0.994	0.369	0.136	0.782

BFS = best-fit sphere; HOAs = higher order aberrationsaDifference in average epithelial thickness along vertical and horizontal meridian within 5-mm diameter. bStandard deviation of central 5-mm epithelial thickness.

TABLE C

ICCs for the Measurements of OCT-based Topographer

	Epithelium-on		Epithelium-off	
Parameter	**ICC**	**95% CI**	**ICC**	**95% CI**
Radius of anterior BFS at 3.5 mm	0.993	0.985 to 0.997	0.996	0.988 to 0.999
Radius of anterior BFS at 6 mm	0.998	0.988 to 0.999	0.998	0.995 to 0.999
Radius of anterior BFS at 9 mm	0.999	0.997 to 0.999	0.999	0.998 to 0.999
Radius of posterior BFS at 3.5 mm	0.994	0.988 to 0.998	0.995	0.989 to 0.998
Radius of posterior BFS at 6 mm	0.999	0.998 to 1.00	0.999	0.997 to 0.999
Radius of posterior BFS at 9 mm	0.999	0.999 to 1.000	0.998	0.997 to 1.000
Anterior asphericity	0.902	0.997 to 1.000	0.871	0.756 to 0.941
HOAs at 3 mm	0.84	0.707 to 0.924	0.788	0.602 to 0.902
HOAs at 6 mm	0.874	0.768 to 0.942	0.917	0.836 to 0.963
Vertex pachymetry	0.813	0.662 to 0.910	0.995	0.90 to 0.998
Axial radius along steepest meridian at 3.5 mm	0.997	0.993 to 0.999	0.992	0.984 to 0.997
Axial radius along flattest meridian at 3.5 mm	0.994	0.987 to 0.997	0.992	0.982 to 0.996
Axis of steepest meridian at 3.5 mm	0.967	0.922 to 0.986	0.884	0.768 to 0.950

ICC = intraclass correlation coefficient; OCT = optical coherence tomography; BFS = best-fit sphere; HOAs = higher order aberrations

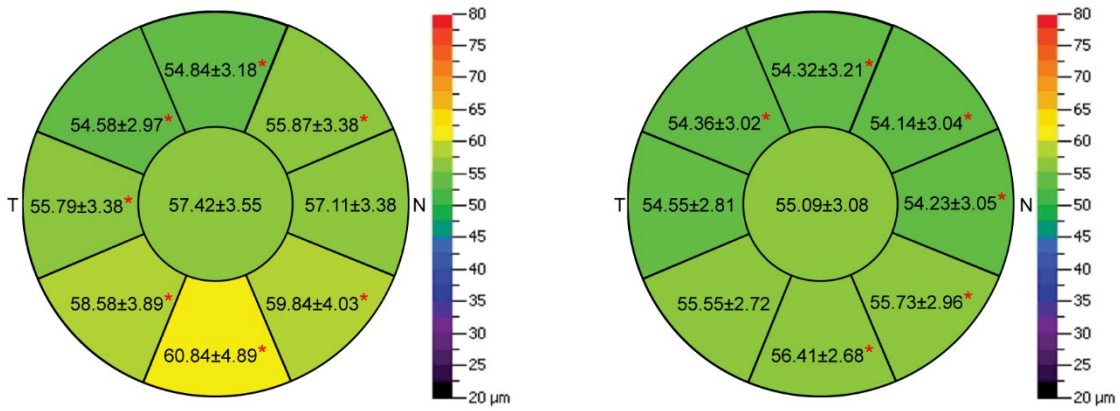

Figure 1. Preoperative epithelial thickness distribution over the central 5-mm diameter in the (Left) main group and (Right) control group.

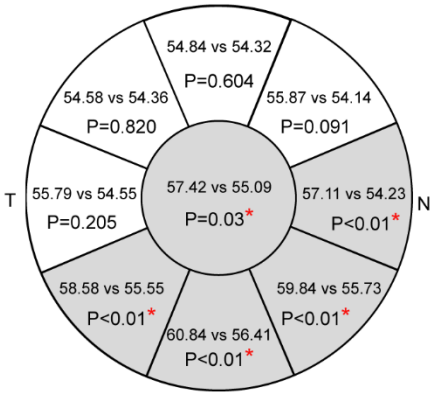

Figure 2. Mean epithelial thickness in eyes with anterior basement membrane dystrophy versus virgin eyes (22 eyes each) with *P* values (red asterisks denote the sections where epithelium in the eyes with anterior basement membrane dystrophy is significantly thicker).

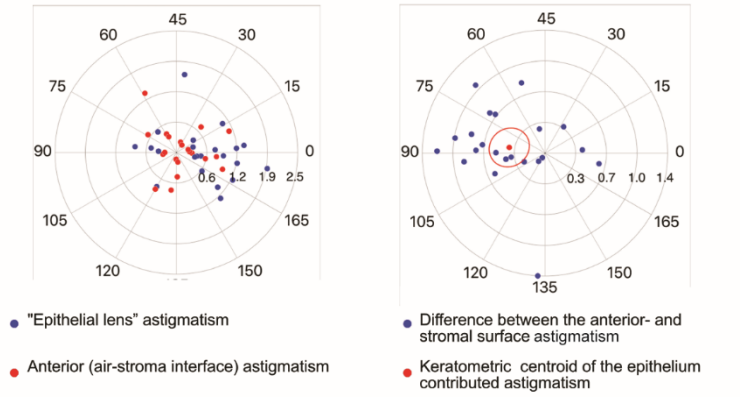

Figure 3. Double-angle plots representing "epithelial lens" astigmatism and stromal surface astigmatism (left) and difference between corneal anterior and stromal surface astigmatism with keratometric centroid of the "epithelial lens" astigmatism (right).

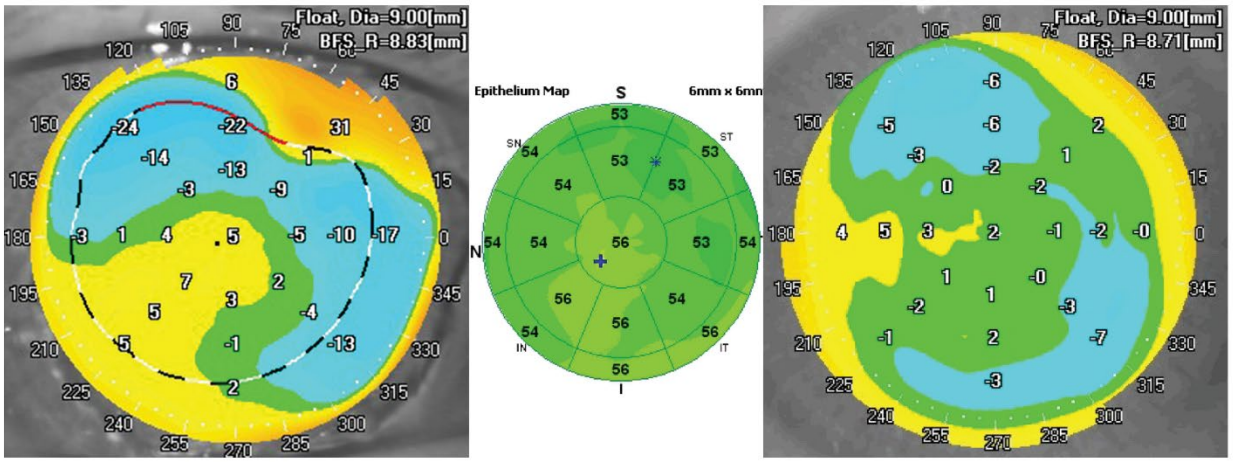

Figure A. Corneal elevation topographies of the same eye before (left) and after (right) epithelial removal, as well as the corneal epithelial thickness map (center) taken before the epithelial removal